Supporting information

Binary Organic Spacer-Based Quasi Two-Dimensional Perovskites with Preferable Vertical Orientation and Efficient Charge Transport for High-Performance Planar Solar Cells

Shi Chen[1†], Nan Shen[1†], Luozheng Zhang[1], Weiguang Kong[1,2], Lihua Zhang[1], Chun Cheng[*1], Baomin Xu[*1]

[1]Department of Materials Science and Engineering, Southern University of Science and Technology, Shenzhen, Guangdong Province, 518055, China
[2]Hebei Key Laboratory of Optic-electronic Information Materials, College of Physics Science and Technology, Hebei University, Baoding, 071002, China

*Correspondence should be addressed to Prof. Chun Cheng and Prof. Baomin Xu (email: chengc@sustc.edu.cn, xubm@sustc.edu.cn)

[†]These authors contributed equally to this work.

Experimental Section

Materials: Methylammonium iodide (MAI), butylammonium iodide (BAI), phenethylammonium iodide (PEAI), Poly(bis(4-phenyl)(2,4,6-trimethylphenyl)amine) (PTAA), [6,6]-phenyl-C_{61}-butyric acid methyl ester (PCBM) and bathocuproine (BCP) were purchased from Xi'an Polymer Light Technology Corp. Lead iodide (PbI_2, 99.9985%) was bought from Alfa Aesar. Solvents including dimethylformamide (DMF), dimethyl sulfoxide (DMSO), isopropanol and chlorobenzene, were purchased from Sigma-aldrich. Patterned indium tin oxide (ITO) glass with a sheet resistance of 15Ω sq^{-1} was bought from Advanced Election Technology Co. Ltd. The perovskite precursor solution was prepared by dissolving PEAI, BAI, MAI and PbI_2 (2-2x : 2x : 3 : 4 molar ratio) in the mixed solvent of DMF and DMSO (9:1 in volume) with concentration of 1.0 M (based on PbI_2).

Device Fabrication: ITO substrates were ultrasonically cleaned with detergent, deionized water, acetone and isopropanol in sequence for 15 min. The pre-cleaned ITO substrates were then treated in a UV cleaner for 20 min. PTAA film was first deposited by spin coating the PTAA solution (0.5 wt% in chlorobenzene) at 6000 rpm for 30s and followed by an annealing step at 100°C for 10 min. For hot-casting perovskite films, the ITO / PTAA substrates were preheated at 100°C for 10 min and then immediately transferred to the spin coater, and the as-prepared perovskite precursor solution was coated onto the ITO / PTAA substrates at a speed of 4000 rpm for 30 s. Subsequently, the substrates were annealed on a hot plate at 100 °C for 10 min. PCBM solution (20 mg/mL in chlorobenzene) was spin-coated at 2000rpm for

30s over the perovskite layer, followed by spin-coating the BCP solution (0.5 mg/mL in isopropanol) at 4000rpm for 30s. Finally, a 100 nm thick silver counter electrode was deposited through a shadow mask by thermal evaporation under a base pressure of 10^{-4} Pa with a device area of 0.1 cm^2.

Characterizations: J-V curves were measured under AM 1.5G one sun illumination (100 mW cm^{-2}) with a solar simulator (Enlitech SS-F7-3A) equipped with a 300 W Xenon lamp and a Keithley 2400 source meter. The light intensity was calibrated by an NREL standard Si solar cell. The external quantum efficiency (EQE) were tested employing an EQE system (Enlitech QE-R3011) including a Xenon lamp, a monochromator, a Si detector for calibration and a dual-channel power. The morphology of perovskite films was characterized by scanning electron microscopy (SEM, TESCAN MIRA3) at a 5 KV accelerating voltage. The surface roughness was characterized by atomic force microscopy (AFM, Bruker Multimode 8-HR). The absorbance spectra were measured by a UV-Vis-NIR spectrometer equipped with an integrating sphere (PerkinElmer Lambda 950). Photoluminescence (PL) and time-resolved PL spectra were recorded by spectrofluorometer (FLS920, Edinburgh instruments), and 405 nm pulsed laser was utilized as excitation source for the time-resolved PL measurements. Proton nuclear magnetic resonance (^{1}H NMR) spectra in $(CD_3)_2SO$ were measured on a Bruker Ascend 500M magnet equipped with BBFO Smartprobe. The routine X-ray diffraction analysis was performed on a Bruker D8 Discover X-ray diffractometer with Cu Kα radiation (1.54Å). Two-dimensional (2D) X-ray diffraction was measured by an HR X-ray diffractometer (Smartlab,

Rigaku) with a 2D detector (PILATUS 100K, Rigaku) operating at 9 kW. The electrochemical impedance spectroscopy (EIS) measurements were performed employing an impedance analyzer (Zahner PP211) in the dark condition. Transient photovoltage was recorded by Zennium workstation (Zahner) equipped with controlled intensity modulated photo spectroscopy system. Electroluminescence (EL) spectra were tested using a Keithley 2614B programmable source meter and a PR670 spectrometer, and the current density-voltage-EQE was measured on a dual-channel Keithley 2614B source meter unit along with a calibrated PIN-25D silicon photodiode. GIWAXS measurements were performed with a Xeuss 2.0 SAXS/WAXS laboratory beamline using a X-ray source and a Pilatus3R 300K detector.

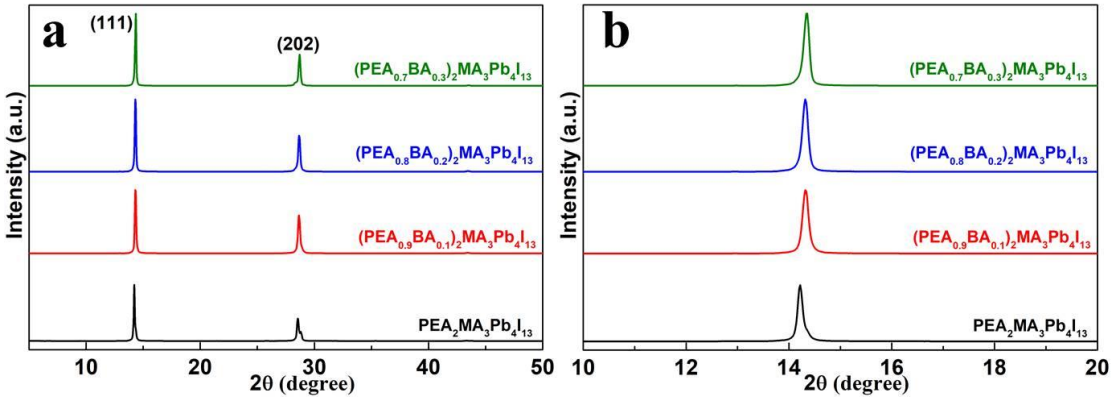

Figure S1 (a) XRD patterns of $(PEA_{1-x}BA_x)_2MA_3Pb_4I_{13}$ binary spacer perovskite films. (b) The magnified XRD peaks between 10° and 20°.

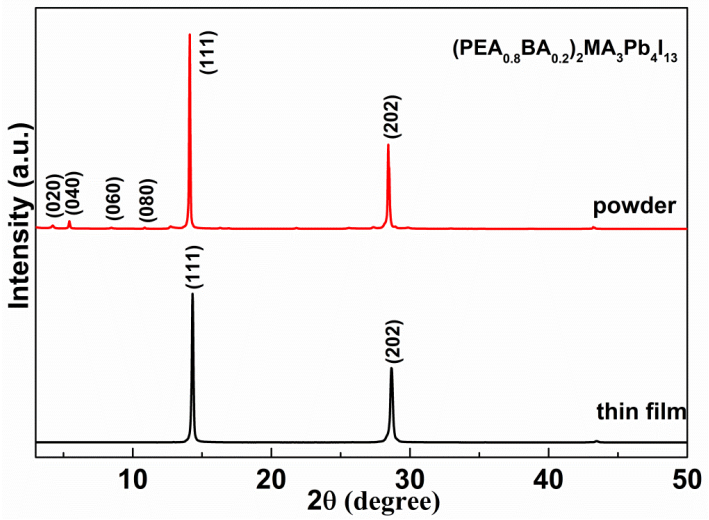

Figure S2 (a) XRD patterns of $(PEA_{0.8}BA_{0.2})_2MA_3Pb_4I_{13}$ perovskite powder (top) and film (bottom), the powder is scraped from oriented films.

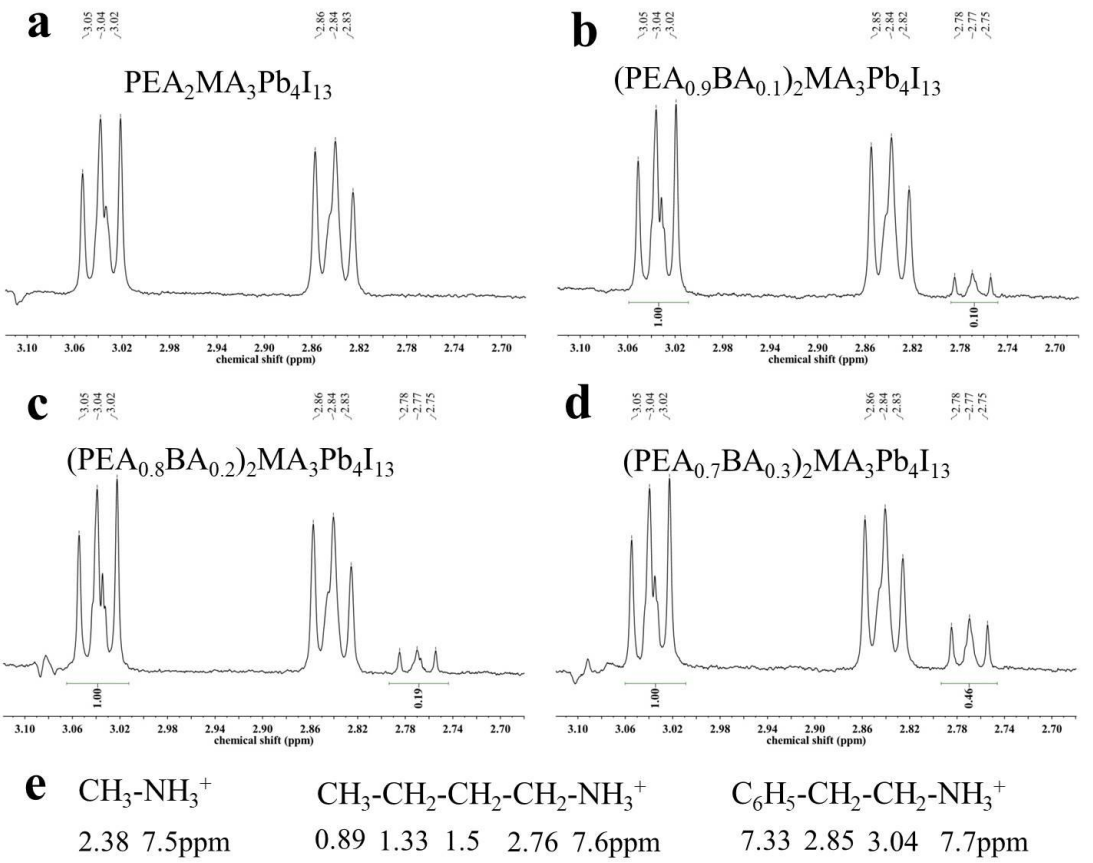

Figure S3 The ^{1}H NMR spectra in the chemical shift of 2.70-3.10 ppm of $(PEA_{1-x}BA_x)_2MA_3Pb_4I_{13}$ binary spacer film, x = 0 (a), 0.1 (b), 0.2 (c) and 0.3 (d). (e) The chemical shift of the H in the three kinds of organic cations.

Figure S3e exhibits the chemical shift of the H in different organic cations. According to our measurement results, we can easily obtain the actual ratio of BA^+ and PEA^+ by comparing the peak of CH_2 in BA^+ (~2.76 ppm) and CH_2 in PEA^+ (~3.04 ppm). The BA spacer concentrations are determined as 9.1%, 16.0% and 31.5% at x = 0.1, 0.2 and 0.3, respectively, close to ratios in the starting materials.

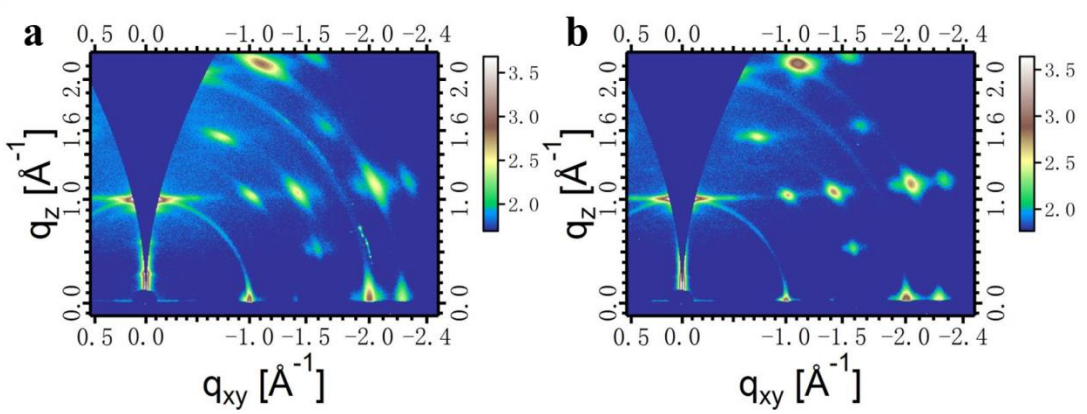

Figure S4 GIWAXS scatting pattern of $(PEA_{1-x}BA_x)_2MA_3Pb_4I_{13}$ films with x = 0 (a) and 0.2 (b), respectively.

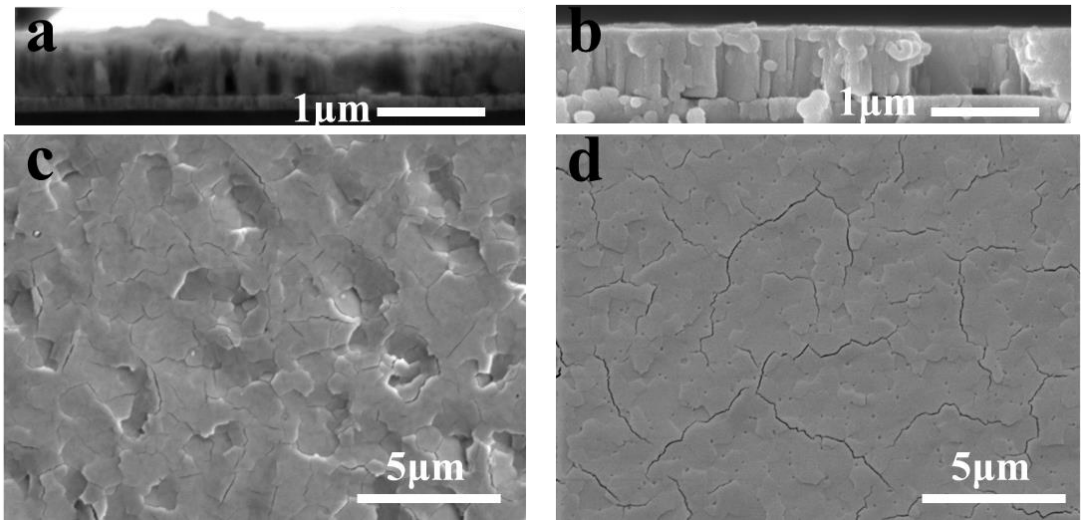

Figure S5 Top view and cross-sectional scanning electron microscopy (SEM) images of $PEA_2MA_3Pb_4I_{13}$ (BA_0) (a, c) and $BA_2MA_3Pb_4I_{13}$ (BA_1)(b, d) perovskite films coated on PTAA substrates, respectively.

In order to elucidate the effect of BA addition on the crystal orientation and the film surface morphology, the SEM images (top view and cross-section), two-dimensional XRD images and AFM images of BA_0 ($PEA_2MA_3Pb_4I_{13}$) and BA_1 ($BA_2MA_3Pb_4I_{13}$) based perovskite films are shown in **Figure S5, S6 and S7**, respectively. Obviously, BA_0 film shows the columnar crystal grains along with the sign of vertical orientation (**Figure S5a**), while the brick-like much larger grains with the significantly increased vertical alignment are observed in BA_1 film (**Figure S5b**). Moreover, two discrete Bragg spots in two-dimensional XRD images become more focused when PEA spacer is replaced with BA spacer (**Figure S6**), further underpinning the enhanced vertical

orientation of crystal grains in BA_1 film. These comparison results indicate that the introduction of BA can facilitate the vertically oriented growth of BA_0 perovskite films.

Besides, the as-obtained much larger crystal grains in BA_1 film can significantly promote the formation of the smoother surface compared to BA_0 film. This is confirmed by the AFM results (**Figure S7**), where we observe an obvious decline of RMS roughness from 26.9 nm (BA_0) to 7.3 nm (BA_1). In addition, the increased vertical orientation of crystal grains in BA_1 film is also helpful to the formation of the smooth surface. The above analysis suggests the BA addition can also favor the formation of the smooth surface of BA_0 based films.

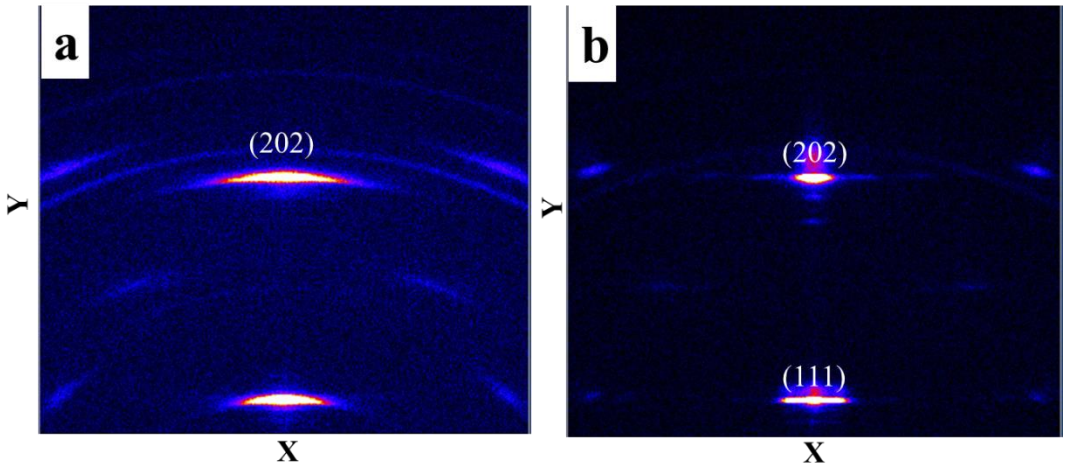

Figure S6 Two-dimensional XRD images of $PEA_2MA_3Pb_4I_{13}$ (a) and $BA_2MA_3Pb_4I_{13}$ (b) perovskite films coated on PTAA substrates, respectively.

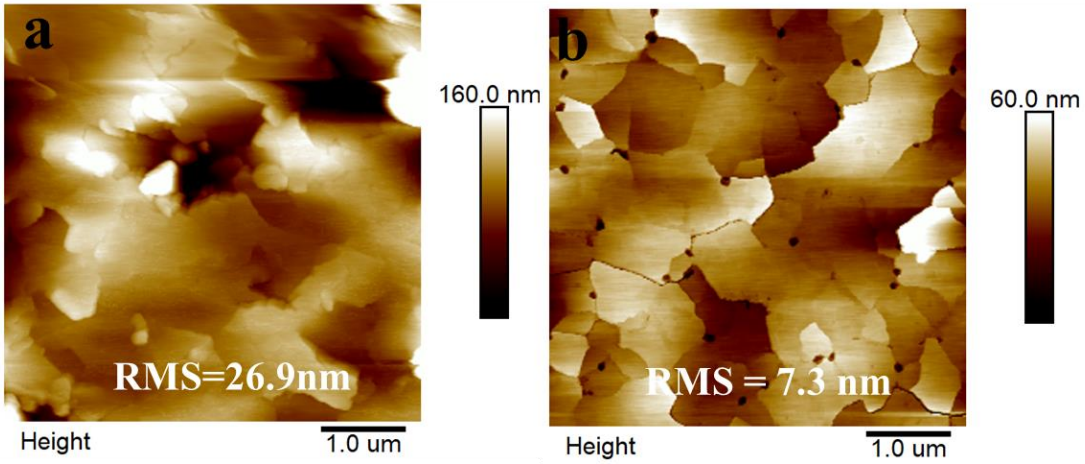

Figure S7 Atomic force microscopy images (size: 5μm×5μm) of $PEA_2MA_3Pb_4I_{13}$ (a) and $BA_2MA_3Pb_4I_{13}$ (b) perovskite films coated on PTAA substrates, respectively.

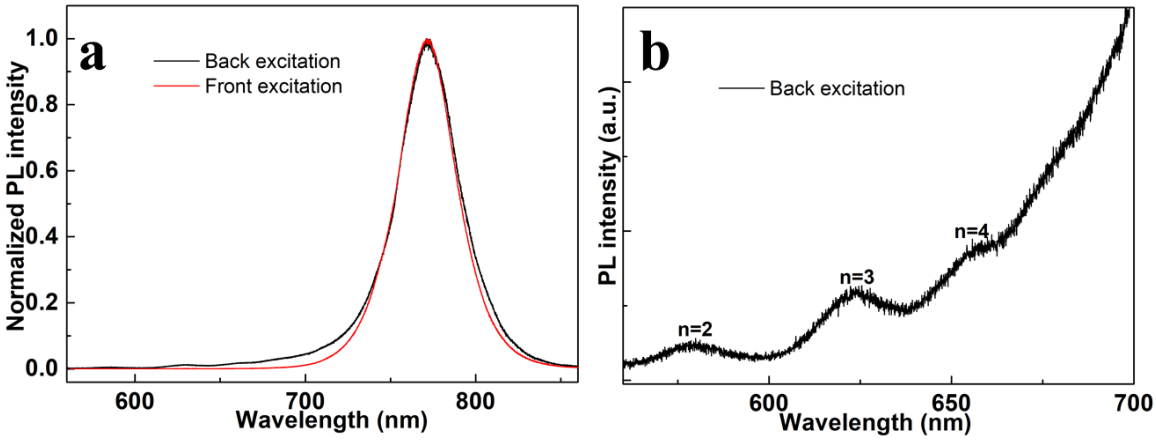

Figure S8 (a) Normalized photoluminescence (PL) spectra of $(PEA_{0.8}BA_{0.2})_2MA_3Pb_4I_{13}$ film excited from the front side (perovskite film) and back side (glass substrate). (b) The magnified PL spectra in the range of 560-700 nm excited from the back side.

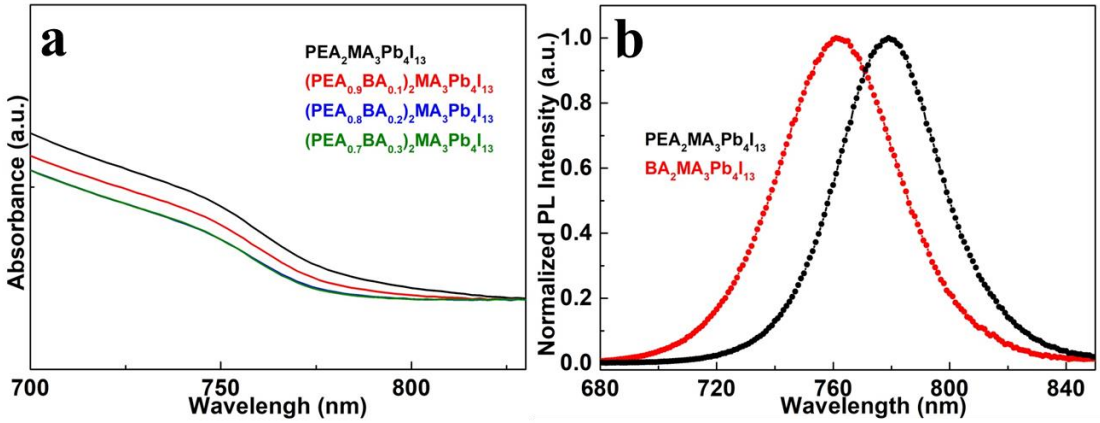

Figure S9 (a) Magnified absorbance spectra of $(PEA_{1-x}BA_x)_2MA_3Pb_4I_{13}$ binary spacer films. (b) Normalized photoluminescence (PL) spectra of $PEA_2MA_3Pb_4I_{13}$ and $BA_2MA_3Pb_4I_{13}$ films excited from the front side.

Table S1 Summary of fitting parameters from time-resolved PL spectra. The average PL lifetime (τ_{ave}) is calculated via the equation of $\tau_{ave} = (A_1^2\tau_1^2 + A_2^2\tau_2^2) / (A_1\tau_1 + A_2\tau_2)$.

Perovskite films	τ_1 [ns]	A_1	τ_2 [ns]	A_2	τ_{ave} [ns]
$PEA_2MA_3Pb_4I_{13}$	7.29	0.34	432	0.66	283
$(PEA_{0.9}BA_{0.1})_2MA_3Pb_4I_{13}$	4.47	0.26	193	0.74	142
$(PEA_{0.8}BA_{0.2})_2MA_3Pb_4I_{13}$	4.09	0.25	126	0.75	93.9
$(PEA_{0.7}BA_{0.3})_2MA_3Pb_4I_{13}$	4.08	0.21	65.3	0.79	50.4

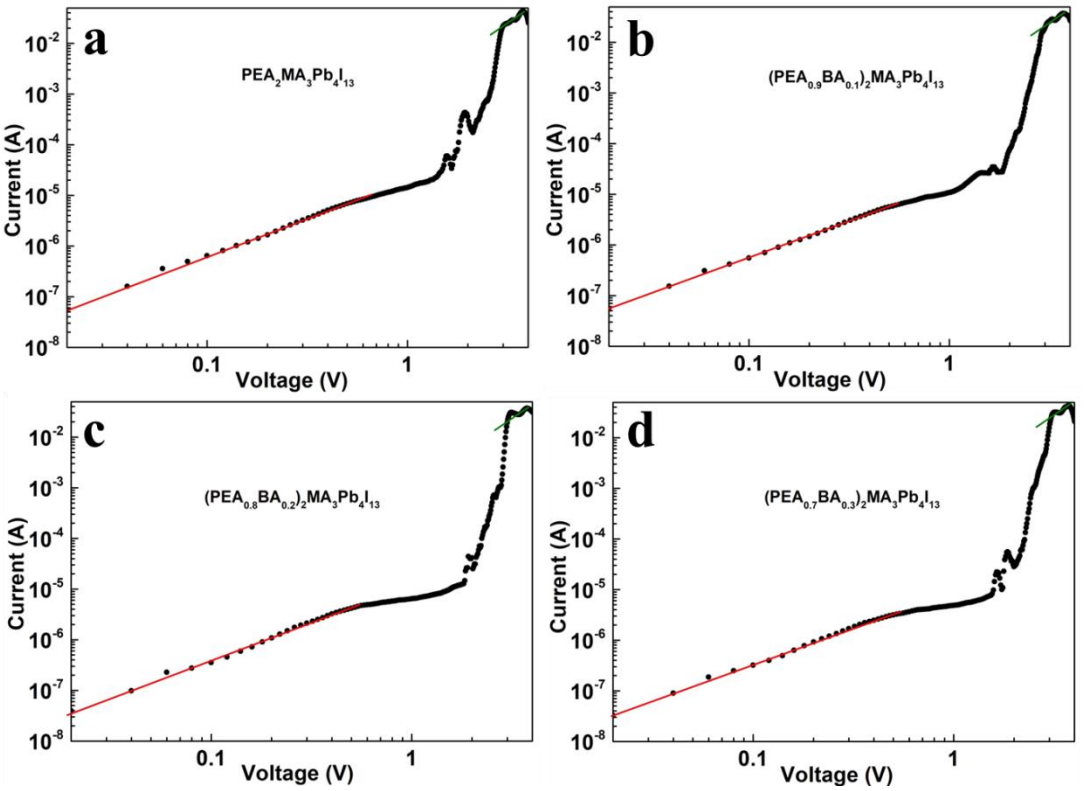

Figure S10 Dark current-voltage characteristics of hole-only Q-2D perovskite device with the active layer of $PEA_2MA_3Pb_4I_{13}$ (a), $(PEA_{0.9}BA_{0.1})_2MA_3Pb_4I_{13}$ (b), $(PEA_{0.8}BA_{0.2})_2MA_3Pb_4I_{13}$ (c) and $(PEA_{0.7}BA_{0.3})_2MA_3Pb_4I_{13}$ (d), respectively. The architecture of hole-only device is ITO / PTAA / Q-2D perovskite / Au. The red and green lines denote the ohmic region ($I \propto V$) and space charge-limited current (SCLC) region ($I \propto V^2$), respectively, and the trap-filled limited region is in between.

The trap density (n_t) can be computed using the equation $n_t = 2\varepsilon\varepsilon_0 V_{TFL} / (qL^2)$, where L is the thickness of perovskite film, ε is relative dielectric constant, ε_0 stands for the vacuum permittivity, q represents the elementary charge and V_{TFL} denotes the onset voltage of the trap-filled limited region.[1] When the hole-only device is operated in the SCLC region, the hole mobility (μ) can be calculated by fitting the equation $J = 9\varepsilon\varepsilon_0\mu V^2 / (8L^3)$, where V is applied voltage and J is dark current.[2]

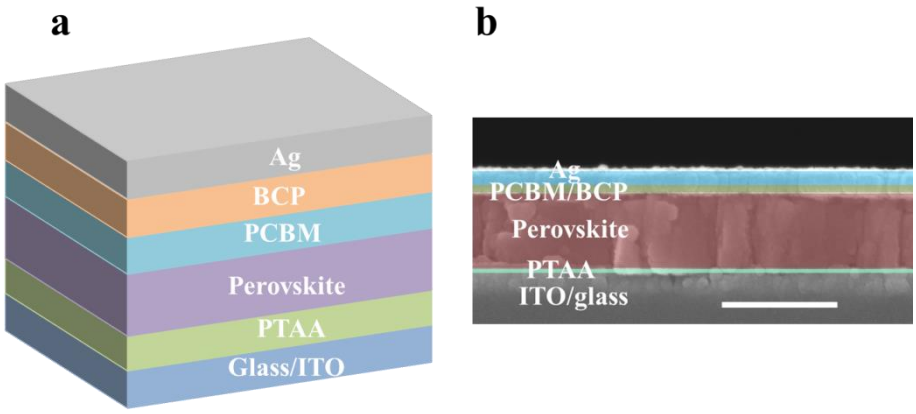

Figure S11 (a) Device architecture of inverted Q-2D perovskite solar cells. (b) Cross-sectional SEM image of a typical $(PEA_{0.8}BA_{0.2})_2MA_3Pb_4I_{13}$ based device. The thickness for each layer is measured to be 20 nm (PTAA), 680 nm (perovskite), 70nm (PCBM and BCP) and 120nm (Ag).

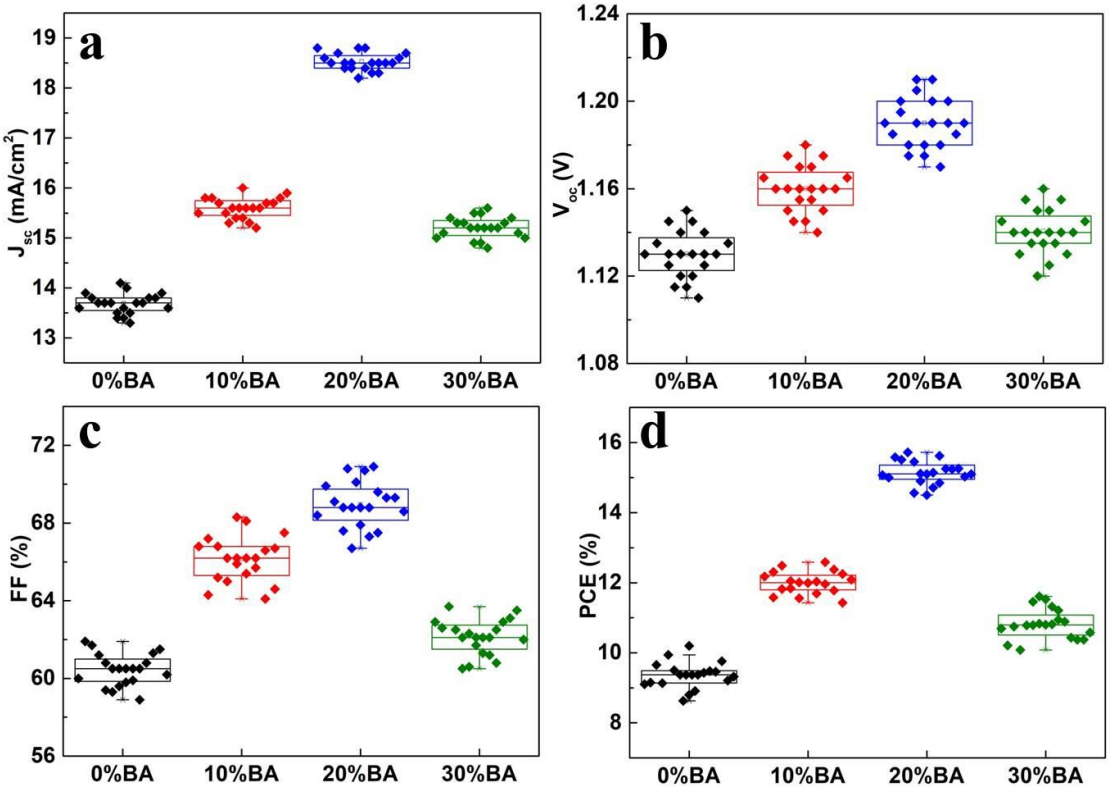

Figure S12 Statistics of photovoltaic parameters obtained from 20 cells.

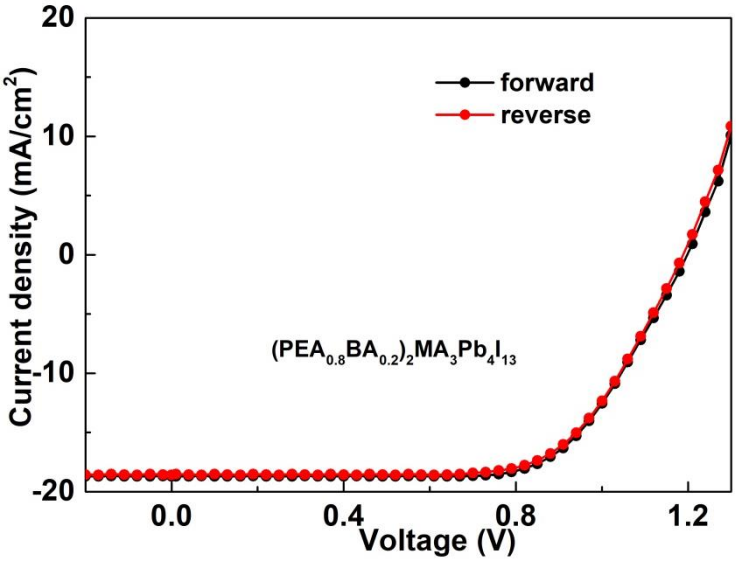

Figure S13 J-V curves of $(PEA_{0.8}BA_{0.2})_2MA_3Pb_4I_{13}$ based binary spacer champion device at the forward and reverse scan directions.

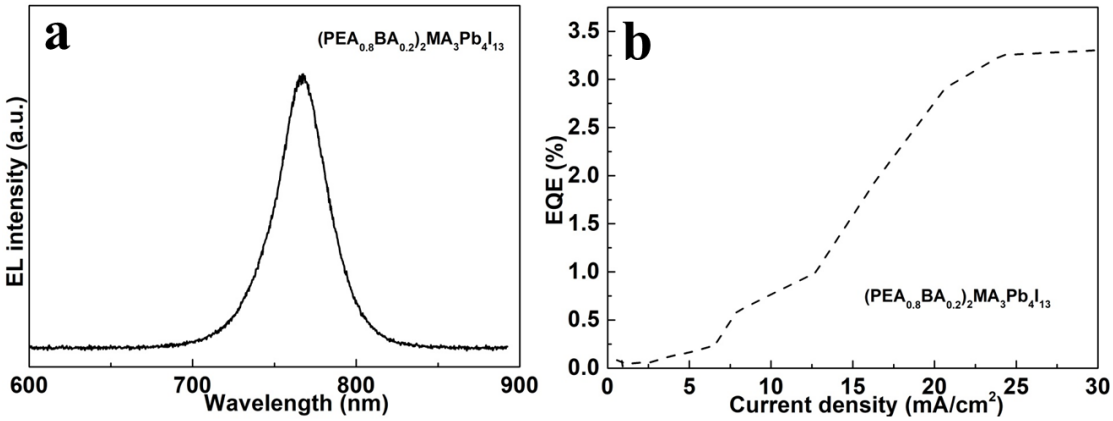

Figure S14 Electroluminescence spectra (a) and EQE spectra (b) of a solar cell acting as a light emitting diode.

1. R. H. Bube, *J. Appl. Phys.*, 1962, **33**, 1733-1737.

2. Q. Dong, Y. Fang, Y. Shao, P. Mulligan, J. Qiu, L. Cao and J. Huang, *Science*, 2015, **347**, 967-970.